

Impact of Dynamic Contrast Enhanced and Diffusion-Weighted MR Imaging on Detection of Early Local Recurrence of Soft Tissue Sarcoma

Bernd M. Erber, MD,^{1*} Paul Reidler, MD,¹ Sophia S. Goller, MD,¹ Jens Ricke, MD,¹ Hans R. Dürr, MD,² Alexander Klein, MD,² Lars Lindner, MD,³ Dorit Di Gioia, MD,³ Tobias Geith, MD,⁴ Andrea Baur-Melnyk, MD,¹ and Marco Armbruster, MD¹

Background: Diagnosis of residual or recurrent tumor in soft-tissue sarcomas (STS) is a differential diagnostic challenge since post-therapeutic changes impede diagnosis.

Purpose: To evaluate the diagnostic accuracy of quantitative dynamic contrast enhanced (DCE)-MRI and diffusion-weighted imaging (DWI) to detect local recurrence of STS of the limb.

Study Type: Prospective.

Population: A total of 64 consecutive patients with primary STS of the limbs were prospectively included 3–6 months after surgery between January 2016 and July 2021.

Field Strength/Sequence: A 1.5 T; axial DWI echo-planar imaging sequences and DCE-MRI using a 3D T1-weighted spoiled gradient-echo sequence.

Assessment: The quantitative DCE-MRI parameters relative plasma flow (rPF) and relative mean transit time (rMTT) were calculated and ADC mapping was used to quantify diffusion restriction. Regions of interest of tumor growth and postoperative changes were drawn in consensus by two experts for diffusion and perfusion analysis. An additional morphological assessment was done by three independent and blinded radiologists.

Statistical Test: Unpaired *t*-test, ROC-analysis, and a logistic regression model were applied. Interobserver reliability was calculated using Fleiss kappa statistics. A *P* value of 0.05 was considered statistically significant.

Results: A total of 11 patients turned out to have local recurrence. rPF was significantly higher in cases of local recurrence when compared to cases without local recurrence (61.1–4.5) while rMTT was slightly and significantly lower in local recurrence. ROC-analysis showed an area under the curve (AUC) of 0.95 (SEM ± 0.05) for rPF while a three-factor multivariate logistic regression model showed a high diagnostic accuracy of rPF ($R^2 = 0.71$). Compared with morphological assessment, rPF had a distinct higher specificity and true positive value in detection of LR.

Data Conclusion: DCE-MRI is a promising additional method to differentiate local recurrence from benign postoperative changes in STS of the limb. Especially specificity in detection of LR is increased compared to morphological assessment.

Evidence Level: 1

Technical Efficacy: Stage 2

J. MAGN. RESON. IMAGING 2023;57:622–630.

Soft-tissue sarcoma (STS) of the limb is a rare entity with an annual incidence of 1 per 100,000 in Europe.¹ STS arises from undifferentiated mesenchymal stem cells and can be divided into various histological categories. Among soft-tissue sarcomas, the most frequent morphology is leiomyosarcoma, while liposarcoma is the most common type

View this article online at wileyonlinelibrary.com. DOI: 10.1002/jmri.28236

Received Feb 12, 2022, Accepted for publication May 5, 2022.

*Address reprint requests to: B.E., Marchioninstr. 15, D-81377 Munich, Germany. E-mail: b.erber@med.uni-muenchen.de

From the ¹Department of Radiology, University Hospital, LMU Munich, Munich, Germany; ²Department of Orthopaedics and Trauma Surgery, Musculoskeletal University Center Munich (MUM), University Hospital, LMU Munich, Munich, Germany; ³Department of Medicine III, University Hospital, LMU Munich, Munich, Germany; and ⁴Department of Interventional Radiology, Klinikum rechts der Isar, Technical University of Munich, Munich, Germany

This is an open access article under the terms of the [Creative Commons Attribution](https://creativecommons.org/licenses/by/4.0/) License, which permits use, distribution and reproduction in any medium, provided the original work is properly cited.

in the limb accounting for approximately 23%.¹ For diagnosis, treatment, and follow-up, a multidisciplinary approach is obligatory. Both therapy and prognosis highly depend on the initial tumor stage, which is commonly assessed according to the current Union for International Cancer Control stage classification system.² Surgery is the standard treatment in all patients. Neoadjuvant chemotherapy (ChT), radiation therapy (RT), and regional hyperthermia (RHT) are recommended in addition to surgery for deep seated STS (>5 cm) with fascial infiltration or dedifferentiated tumors.^{3–6} In these cases, surgical resection is followed by adjuvant radiation therapy to prevent local recurrence (LR).^{3,7}

The risk of LR is very dependent on intrinsic factors like tumor size and tumor entity, as well as extrinsic factors like multifocally positive margins.⁸ Overall, after a follow-up of 24 months, the rate for LR is estimated to be as high as 16%.⁹ Follow-up is usually performed every 3–4 months during the first 2–3 years, every 6 months during the 4–5 years, and once a year after that.^{2,10} For the follow-up, usually CT is used to screen for lung metastases and MRI is used for the detection of LR following the recommendations of the American College of Radiology Appropriateness Criteria guidelines.¹¹

Since pronounced post-therapeutic changes like muscular and subcutaneous edema are present in the area of surgery in the early follow-up, and scar tissue is formed in the further course, an imaging-based distinction between post-therapeutic changes and LR is often difficult to achieve because of similar imaging findings like contrast enhancement.^{12,13} These difficulties may lead to a delayed therapy in false negative cases or unnecessary biopsies in false positive cases. Reliable detection and characterization of early recurrences are therefore mandatory.

Two prior studies have shown the potential of dynamic contrast enhancement (DCE) to help in the differential diagnosis of LR in STS vs. post-therapeutic changes, although both studies did not use quantitative DCE-MRI and images were only analyzed visually.^{14,15} Also, radiomics models have shown previously that DCE-MRI might even

contain prognostic information.¹⁶ In this study, we aimed to test the hypothesis whether quantitative DCE-MRI allows for the detection of tumor recurrence in patients with STS and post-therapeutic changes as this method generates objective values basically independent of subjective assessment.

Materials and Methods

Patients

Approval of the local institutional review board (Nr. 17-279) and written informed consent from all participants were obtained for this prospective study.

Inclusion criteria for this study included participants with STS of the limb (grade 2 and 3) who had undergone surgery in our university or in another hospital and afterward have been sent to our orthopedic department for further treatment. Exclusion criteria are shown in Fig. 1. Between January 2016 and July 2021, 64 participants with STS of the limb meeting the study eligibility criteria were included. As seen in Table 1, most participants received neoadjuvant ChT and RHT before surgical excision of the tumor, followed by RT, ChT, and RHT (40/64) after surgical excision. Routine follow-up, which consisted of MRI, DCE-MRI, and clinical assessment of the site of tumor excision, was done every 3 months in the first 3 years and then every 6 months in years 4 and 5.

Assessment of STS Local Recurrence

Reference standard was histology in all 11 cases of LR, and follow-up MRI in all 53 patients without clinical or radiological signs of LR. Reference standard for follow-up imaging had to show marked resolution of signal changes after at least 6 months without evidence of tumor growth, which was interpreted by an expert in musculoskeletal imaging with more than 20 years of experience and a resident with 3 years of experience in radiology (A.B.M., B.E.).

MRI Data Acquisition

MRI studies were performed on a 1.5 T magnet (Avanto; Siemens Healthineers; Erlangen; Germany). Precontrast sequences included coronal STIR sequences, axial and coronal T1-weighted, axial T2-weighted TSE and axial diffusion-weighted (DWI) echo-planar imaging (EPI) sequences. Postcontrast sequences included axial and coronal T1-weighted fat saturated images after DCE-MRI.

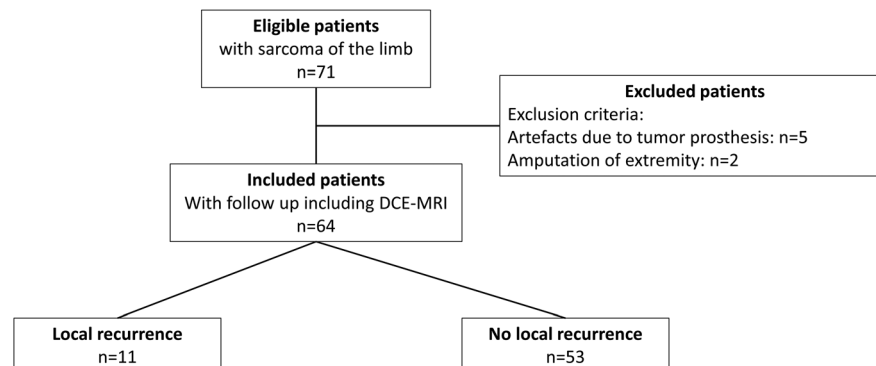


FIGURE 1: Flow chart diagram showing number of included and excluded patients with and without local recurrence.

	LR	No LR
Sex		
f	4	23
m	7	30
Age		
Mean	67	62
Histopathological subtype		
Synovial sarcoma monophasic		3
Synovial sarcoma biphasic		2
Pleomorphic sarcoma	4	26
Leiomyosarcoma	1	6
Liposarcoma	1	8
Myxofibrosarcoma	2	2
Malignant peripheral nerve sheath tumor	2	2
Spindle cell sarcoma	1	0
Other	0	4
Primary tumor site		
Thigh and waist	6	34
Lower leg	3	7
Forearm		6
Upper arm	2	5
other		1
Grading		
G2	3	23
G3	8	30
Therapy neoadjuvant		
≥4 cycles Doxorubicine/ Ifosfamide + RHT	3	25
<4 cycles Doxorubicine/ Ifosfamide + RHT	1	11
8cycles EIA		1
No neoadjuvant therapy	7	16
Therapy adjuvant		
≥4 cycles Doxorubicine/ Ifosfamide + RHT + RT	7	10
≥4 cycles Doxorubicine/ Ifosfamide + RHT	3	15

TABLE 1. Continued

	LR	No LR
<4 cycles Doxorubicine/ Ifosfamide + RHT + RT		7
Only RT	1	5
≥4 cycles Doxorubicine/ Ifosfamide + RT		1
other		15

Table showing various patient characteristics including histological subtype of the sarcoma and neoadjuvant and adjuvant therapy (f = female; m = male; RHT = regional hyperthermia; RT = radiotherapy).

DIFFUSION-WEIGHTED IMAGING PARAMETERS. Imaging parameters of DWI were as follows: repetition time/echo time 5600/71 msec; matrix 192×144 ; slice thickness 5 mm; field-of-view: $400 \times 300 \text{ mm}^2$; b-values 50 sec/mm^2 and 800 sec/mm^2 .

DYNAMIC CONTRAST-ENHANCED IMAGING PARAMETERS. DCE-MRI data were acquired using a 3D T1-weighted spoiled gradient-echo sequence that was accelerated using view sharing and parallel imaging (time-resolved angiography with stochastic trajectories [TWIST]). Imaging parameters of DCE-MRI were as follows: repetition time/echo time 2.37/0.83 msec; flip angle 15° ; matrix 192×192 ; parallel acquisition acceleration factor 4 with a generalized auto-calibrating partially parallel acquisition algorithm (GRAPPA) with 24 reference lines; number of slices 48; slice thickness 4 mm; phase/slice oversampling 17%/25%; field of view $400 \times 400 \text{ mm}^2$; phase/slice resolution 100%/63%; partial Fourier 7/8; central TWIST region A 20%; and TWIST sampling density B 25%. Total acquisition of DCE-MRI was 5 minutes. Temporal resolution was 2.2 seconds per 3D-volume. A contrast agent dose of 0.1 mL/kg of Gadobutrol (Gadovist, Bayer Healthcare, Germany) was injected 10 seconds after starting the acquisition via an antecubital vein with a flow of 2 mL/sec and flushed with 30 mL saline at the same rate.

MRI and DCE-MRI Postprocessing

All DCE-MRI data were postprocessed using PMI 0.4 (Platform for Research in Medical Imaging) and written in-house software in IDL6.4 (ITT, Boulder, CO). Contrast agent concentrations were approximated by the relative signal enhancement $S(t)/S_0 - 1$, where $S(t)$ is the postcontrast signal intensity at time t and S_0 is the precontrast baseline signal intensity.^{17,18} Arterial and venous blood concentrations were converted to plasma concentrations using a standardized hematocrit of 0.48. The arterial input function (AIF) was defined within the lumen of the largest artery on the level of the tumor, depending on the site of imaging. To select only the voxels contained within the arteries, these regions of interest (ROI) were shrunk automatically by selecting the pixels in the top 10% of the value range as it was done in previous studies.¹⁸ Semi-quantitative maps for plasma flow and mean transit time were calculated by deconvolution of tissue concentrations with the arterial input function.^{17,19}

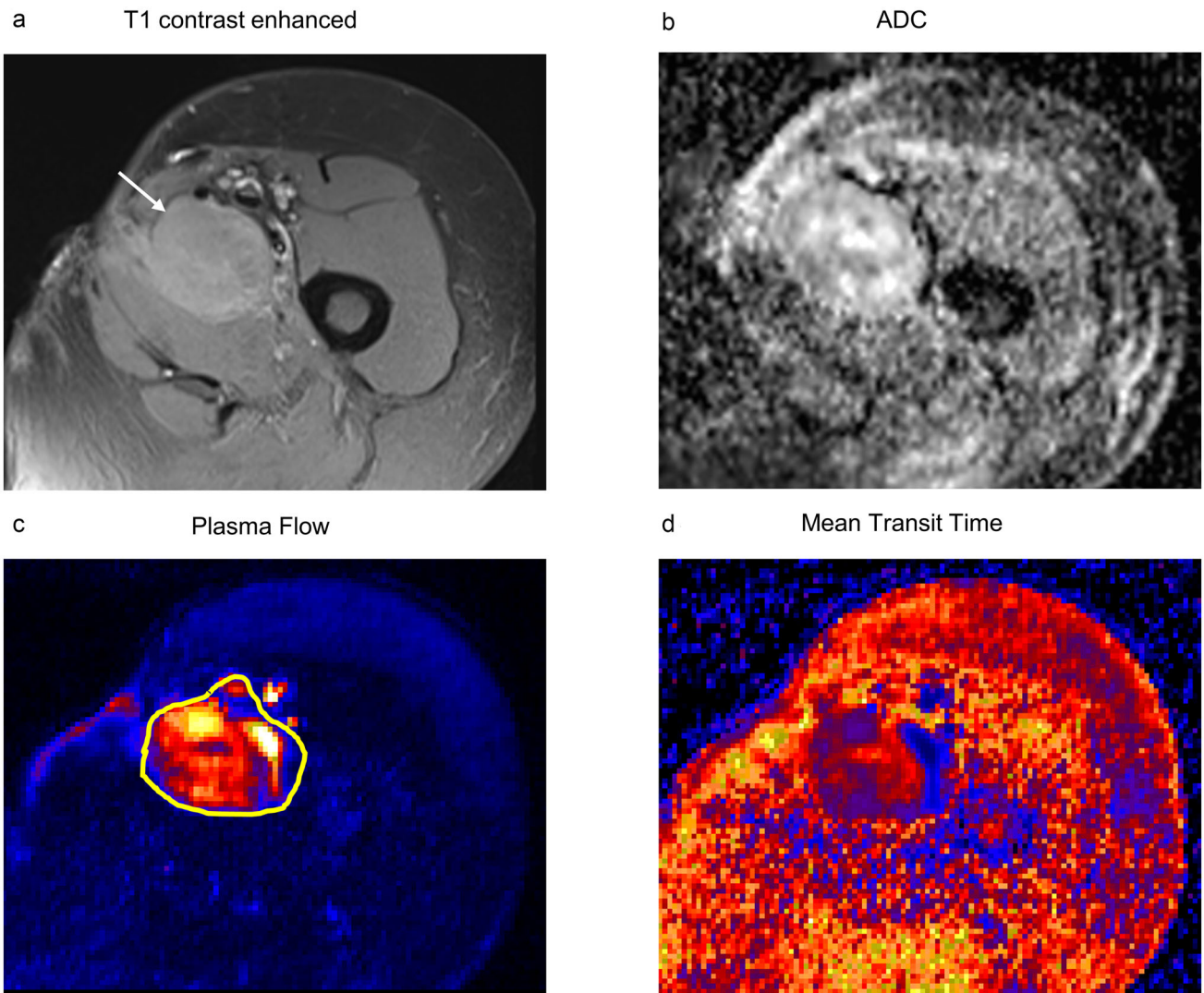


FIGURE 2: Images of a 70-year-old patient with G3 liposarcoma and local recurrence of STS in the groin. (a) Contrast-enhanced T1-weighted image. White arrow shows slight enhancement of the lesion. (b) ADC-map. (c) Plasma flow. In local recurrence, plasma flow is markedly increased compared to surrounding tissue; (d) mean transit time in local recurrence is slightly decreased.

Definition of Regions of Interest

In cases with LR, ROIs for ADC-mapping and DCE-MRI were drawn covering the whole tumor in the slice where the lesion showed its greatest extension. As reference, a ROI of the same size and shape was drawn in healthy tissue of the opposite side to calculate relative values of PF and MTT, which are better comparable (rPF and rMTT). In patients without LR, a ROI was drawn in the area of resection with the strongest contrast enhancement on conventional T1-w images, as shown in Figs. 2 and 3. According to LR, a ROI of the same size and shape was drawn in healthy tissue of the opposite side to calculate relative values, respectively.

ROIs were drawn in consensus by an expert in musculoskeletal imaging with more than 20 years of experience and a resident with 3 years of experience in radiology (A.B.M., B.E.).

Morphological MRI Assessment

Furthermore, standard images were visually interpreted by three separate readers, one radiology resident with 4 (S.G.) and two

board-certified radiologists with 6 (P.R.) and 7 (M.A.) years of experience in tumor imaging. Readers were blinded for clinical outcome data, as well as the DCE results and radiologic report. For morphological assessment, readers used STIR, T1-weighted and T2-weighted TSE precontrast sequences as well as T1-weighted fat saturated images after intravenous contrast. Lesions were systematically classified on a 5-point Likert scale applying the following lesion classification: 1—definitely benign; 2—probably benign; 3—intermediate risk for malignancy – short-term follow-up or biopsy needed; 4—probably malignant; 5—definitely malignant; 1 and 2 were grouped and rated as correct identification of No-LR and 3–5 were grouped and rated as correct identification of LR or in need of clarification.

Statistical Analysis

Statistical analysis was performed using SPSS (IBM; Armonk, NY) and R-Studio (Version 4.0.4, RStudio Inc., Boston, MA). Relative values of PF and MTT were calculated for each patient by dividing the absolute values of PF/MTT in the area of resection by the

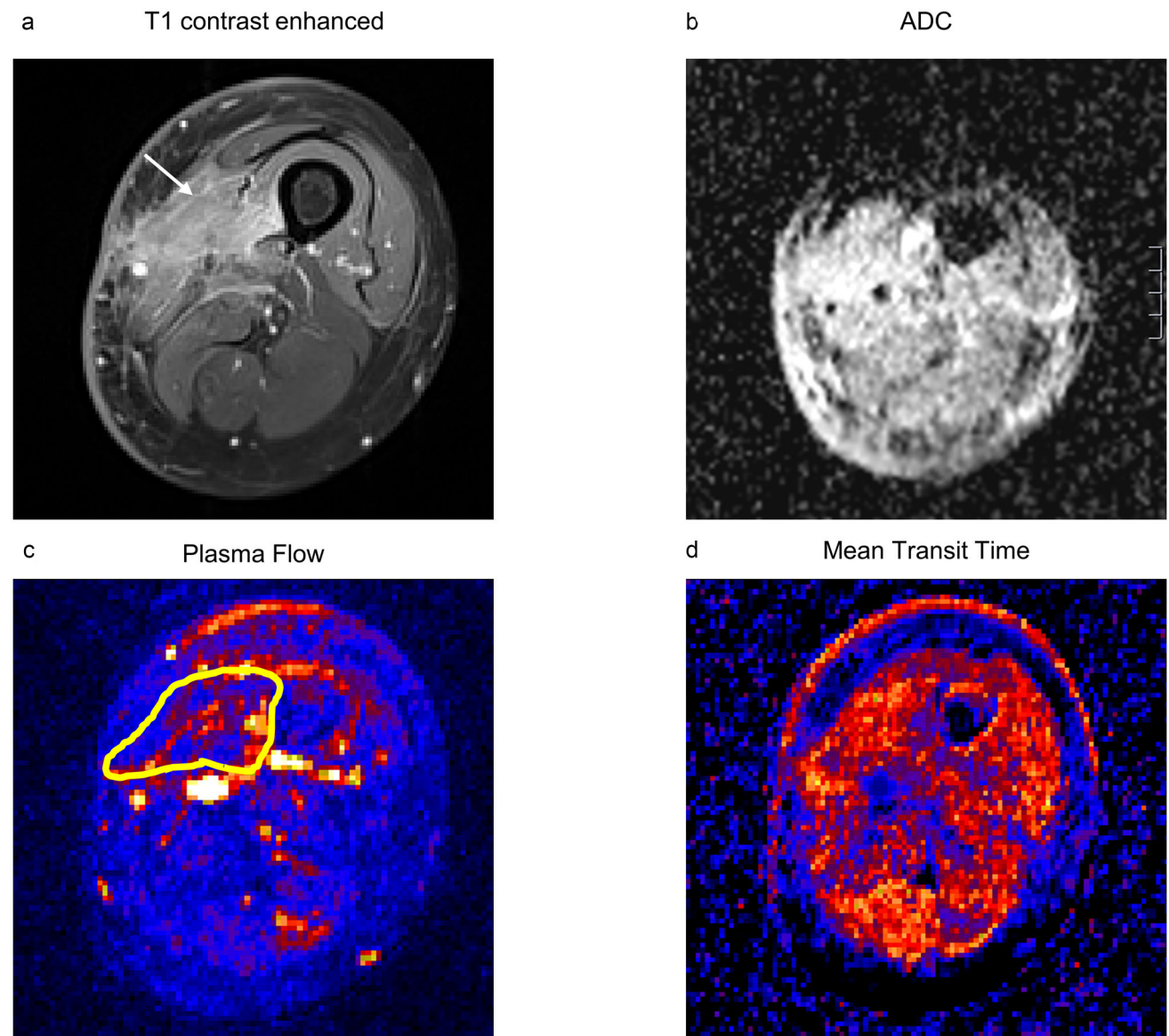


FIGURE 3: Regular postoperative situs of the thigh of a 52-year-old woman after excision of pleomorphic sarcoma. No Recurrence was detected in routine follow-up 6 months later. (a) Contrast-enhanced T1-weighted image. White arrow shows slight enhancement. (b) ADC-map. (c) Plasma flow map. PF is minimally increased in the area of surgery compared to surrounding tissue. (d) Mean transit time map. It shows no relevant change in the area of surgery compared to surrounding tissue.

absolute values of PF/MTT of healthy tissue (rPF and rMTT). Student's *t*-test for independent samples was used to examine whether rPF, rMTT, and ADC variables were different between patients with LR and patients with benign postoperative changes (No-LR). Receiver operating characteristic (ROC) curves were plotted to analyze the diagnostic ability of rPF, rMTT, and ADC. In a multivariable logistic regression model, we tested for incremental values of using more than one perfusion parameters. Sensitivity, specificity, true positive, and negative rate were calculated for each reader and Fleiss kappa statistics were evaluated for interobserver reliability. The degree of agreement was classified using kappa values according to the recommendation by Landis and Koch²⁰ as follows: 0.21–0.40 fair agreement; 0.41–0.60 moderate agreement; 0.61–0.80, substantial agreement; 0.81–1.00, almost-perfect agreement. The limit of significance was set to 0.05, resulting in 95% confidence intervals (CIs).

Results

Patients

Out of the 64 patients meeting the study eligibility criteria, 11 showed LR in routine follow-up, while 53 patients had no LR in routine follow-up (Fig. 1). Mean patient age in the LR group was 67 years and 62 years in the No-LR group. Most common histological subtype in both groups was pleomorphic sarcoma (4/11 in LR patients and 26/53 in No-LR patients). The thigh was the most common tumor site for both groups. Mean time (min–max, standard error of mean [SEM]) between surgery and detection of LR in MR imaging was 27.1 (3.4–87.8, ± 5.8) months, while between surgery and corresponding follow-up was 28.9 (3.1–90, ± 3.4) months in the group of No-LR.

TABLE 2. Comparison of rPF and Morphological Assessment

	Sensitivity	Specificity	TPR	TNR
rPF	91.0	88.8	62.5	97.9
Reader 1	100.0	67.9	39.3	100.0
Reader 2	91.0	73.6	41.7	97.5
Reader 3	72.7	54.7	25.0	90.6

Table showing sensitivities, specificities, true positive rate (TPR) and true negative rates (TNR) for rPF and three blinded readers.

ADC Mapping Parameter

The mean ADC value (min–max, SEM) for lesions, which were histologically proven to be LR was 1.35 mm²/sec (1.03–1.78 mm²/sec, ± 0.09 mm²/sec), while for No-LR was 1.55 mm²/sec (0.96–2.47 mm²/sec, ± 0.06 mm²/sec). *t*-test showed no significant differences between ADC values of LR and No-LR, as seen in Fig. 4 (*P* = 0.21). ROC-analysis resulted in an area under the curve (AUC) of 0.62 (SEM ± 0.08) (Fig. 5).

DCE-MRI Parameters

PLASMA FLOW. Mean PF (min–max, SEM) for in postoperative tissue with No-LR was 36.9 mL/min per 100 mL (1.7–238.7, ± 8.7) with a mean rPF of 4.5 (0.5–20.3, ± 0.6) compared to not affected tissue, respectively.

Mean PF in lesions with LR was 223.2 mL/min per 100 mL (8.8–290.5; ± 114.4) with a rPF of 61.1 (4.3–81.0; ± 12.6). *t*-test showed that rPF values of LR were significantly higher than of No-LR (Fig. 4). ROC-analysis resulted in an AUC of 0.95 (SEM ± 0.04; Fig. 5). An optimum cutoff

value was calculated at a rPF value of 6.74 (sensitivity: 90.9%; specificity: 86.8%).

EXTRACELLULAR MEAN TRANSIT TIME. Mean MTT (min–max, SEM) for No-LR was 58.3 sec (9.4–150.6; ± 4.6 sec) with a relative MTT of 0.9 (0.2–4.3; ± 0.1) compared to not affected tissue, respectively. Mean MTT in lesions proved to be LR was decreased to 37.8 sec (7.0–97.1; ± 8.4 sec) and 0.5 times the values of not affected tissue (0.04–1.5; ± 0.1). Difference between rMTT of LR and No-LR patients was statistically significant (Fig. 4). ROC-analysis resulted in an AUC of 0.77 (SEM 0.09; Fig. 5). An optimal cutoff value was calculated at a rMTT value of 0.61 (sensitivity: 72.7%; specificity: 77.4%).

Multivariate Logistic Regression Analysis

A three-factor multivariate logistic regression model for the combination of both DCE-MRI parameters and ADC was implemented. Analysis showed a high diagnostic accuracy to evaluate the presence or absence of LR using rPF (*R*² = 0.71; odds ratio 1.17). rMTT and ADC did not contribute significantly to the model (*R*² combining rPF, rMTT and ADC = 0.78; *P* = 0.76).

Comparison to Morphological Assessment

Distribution of Likert scale rating was 5-31-17-7-4 (for Likert 1-2-3-4-5) for reader 1, 2-38-12-9-3 for reader 2, and 4-28-13-14-5 for reader 3.

Reader 1 had a sensitivity of 100% (11/11 patients with LR) for identification of LR (correct identification of LR; Likert 3–5), reader 2 a sensitivity of 90.1% (10/11), and reader 3 a sensitivity of 72.7% (8/11). Specificity (correct identification of No-LR; Likert 1 and 2) was 67.9% for reader 1 (36/53 patients with No-LR), 73.6% (39/53) for reader 2 and 54.7% (29/53) for reader 3. True positive rate (and true negative rate) was 39.3% (100%) for reader 1, 41.7% for reader 2 (97.5%), and 25.0% (90.1%) for

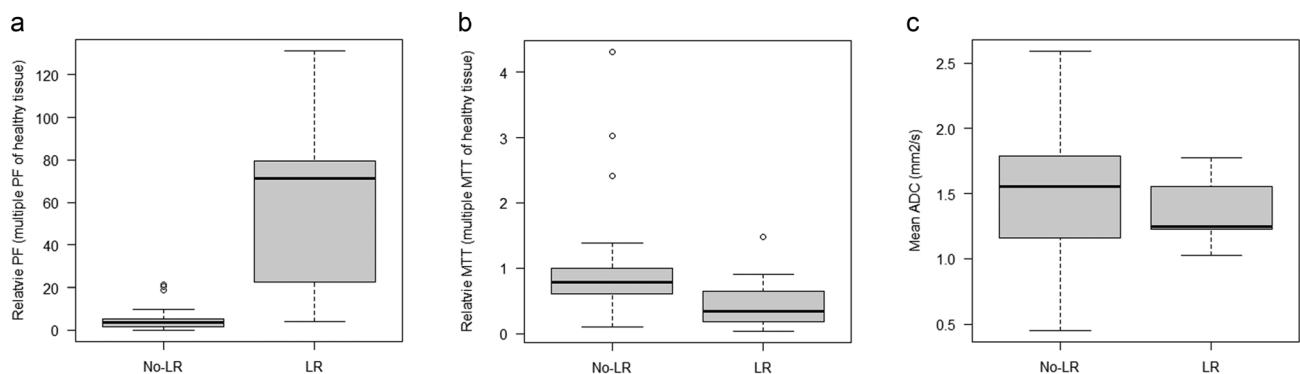


FIGURE 4: Boxplots showing minimum, first quartile, median, third quartile and maximum for (a) relative plasma flow (rPF) (0.08, 1.56, 3.55, 5, 27, 21, 25 in No-LR and 4.27, 22.57, 71.50, 79.77, 131.25 in LR), (b) relative mean transit time (rMTT) (0.11, 0.61, 0.78, 1.00, 4.31 in No-LR and 0.04, 0.19, 0.35, 0.65, 1.48 in LR), and (c) mean ADC (in mm²/sec) (0.45, 1.61, 1.56, 1.79, 2.59 in No-LR and 1.02, 1.23, 1.25, 1.56, 1.78 in LR) for local recurrence (LR) and no local recurrence (No-LR) patients. Differences were significant for rPF and rMTT but not for mean ADC.

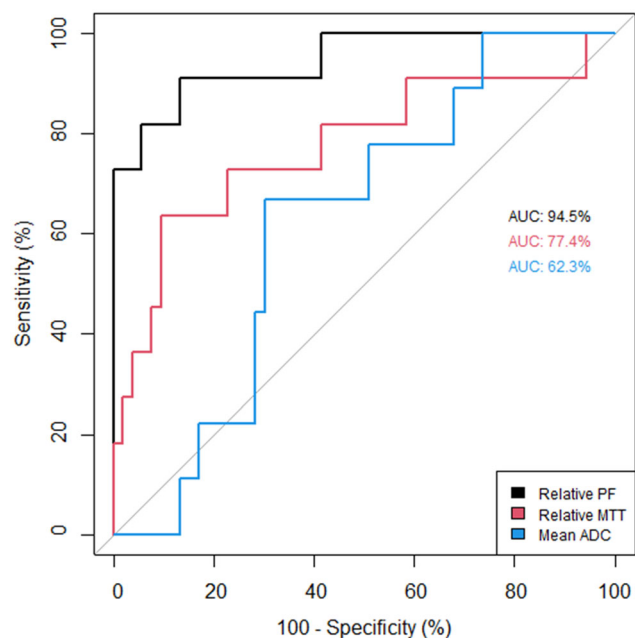


FIGURE 5: ROC graphs showing AUCs for relative plasma flow (black), relative mean transit time (red) and mean ADC (blue) based on the presence of local recurrence and no local recurrence.

reader 3 (Table 2). In patients with No-LR who were wrongly assessed for possible recurrence by the readers (false positive, Likert 3–5), rPF was true negative referring our optimal cutoff in 94.1% (16/17 patients) for reader 1, 92.9% (13/14) for reader 2 and 83.3% (20/24) for reader 3.

Reader 1 assigned intermediate risk for malignancy and the need of short-term follow-up or biopsy (Likert 3) in 17 cases, reader 2 in 12 cases and reader 3 in 13 cases as mentioned above. For intermediate risk assessment Likert 3, we found 2 LR and 15 No-LR for reader 1, 1 LR and 11 No-LR for reader 2 as well as 0 LR and 13 No-LR for reader 3.

In these cases, rPF presented correct classification of 1 out of 2 (50%) of LR and 14 out of 15 (93.3%) of No-LR for reader 1, 1/1 (100%) of LR and 11/11 (100%) of No-LR for reader 2 and 0/0 of LR and 11/13 (84.6%) of No-LR for reader 3.

Interobserver reliability was fair with a kappa of 0.26 (95% confidence interval 0.18–0.35).

Discussion

This study aimed to test the hypothesis that quantitative DCE-MRI allows for the detection of local tumor recurrence in patients with STS and post therapeutic changes. In this prospective study with patients after multimodal therapy including surgical resection, 11 out of 64 patients showed LR of STS of the limb. Lesions, which were histologically proven to be LR, showed significantly higher rPF than reactive post-operative changes, also presenting contrast enhancement in

conventional images. The results of a multivariate logistic regression analysis indicated that rPF was a strong predictor of LR in STS of the limb in MR-based diagnosis), while rMTT and ADC had no statistically relevant additional effect. Compared to morphological assessment DCE-MRI performed with distinct higher specificity.

DCE-MRI is a functional MR technique, which allows to get an insight into the perfusion of tissue.^{19,21} Our results are consistent with previous studies investigating the relevance of DCE-MRI. A study published by del Grande et al¹⁵ with a cohort of 37 patients (6 with LR and 31 with No-LR) reported an excellent sensitivity of 100% for the detection of LR with static CE-MRI as well as DCE-MRI for two experienced readers. Interestingly, specificity increased from 52% with CE-MRI to 97% with use of DCE-MRI, which agrees with the results of our study. For interpretation of DCE-MRI, readers used composite maximum intensity projection images as well as images from the individually acquired time phases as qualitative parameters. In our prospective study including 11 patients with LR and 53 patients with No-LR, evaluation and interpretation of DCE-MRI were extended to a quantitative analysis of both parameters PF and MTT.

In this study, differences in mean ADC between LR and post-therapeutic changes in patients with No-LR were not statistically significant, although mean ADC values of LR were slightly below values of post-therapeutic changes in patients with No-LR. This differs from the findings of del Grande et al,¹⁵ who found significant differences in ADC between LR and No-LR (1.08 mm²/sec in LR was significantly different from postoperative scarring with 0.9 mm²/sec). The review of Subhawong and Wilky²² showed that relevance of ADC mapping in imaging of STS and bone sarcomas has been widely discussed in the literature, as various studies showed both the ability and failure of ADC to differentiate between benign and malignant lesions. Wang et al²³ showed that ADC mapping might be of relevance in surveillance after neoadjuvant therapy of bone sarcomas in a study with 35 patients, while Chodyla et al²⁴ observed a significant increase of mean ADC values between responders and nonresponders of neoadjuvant therapy in 37 patients with STS of the limb. On the other side, Hayashida et al²⁵ detected no significant difference in mean ADC values between chondrosarcomas and benign bone masses.

This study analyzed the benefits of DCE-MRI in detection of LR in STS of the limb after multimodal therapy including surgical resection with a prospective setting. Furthermore, it included patients who had undergone neoadjuvant therapy including regional hyperthermia, which has previously shown to increase the benefit of chemotherapy.⁴

In reviewing the literature, only a small benefit in sensitivity of MRI compared to the clinical evaluation or other imaging methods has been reported.^{9,12–15,26} In the study of Labarre et al,¹³ only 2 out of 11 LR were detected with MRI

and they found a relatively poor positive predictive value of 42%. Results of Cheney et al¹² were even more impressive as surveillance MRI could only detect one asymptomatic LR (1/114).

In our study, we found an optimal specificity of 86.8% for rPF, which was distinctly higher than specificity of readers using only morphological MRI sequences while sensitivity was similar. Furthermore, rPF detected most (83.3%–94.1%) of false positive rated MRIs as true negative. These results claim a benefit of DCE-MRI in surveillance of LR in STS according to the findings of del Grande et al,¹⁵ which showed an increase of readers specificity from 52% to 97% with the additional use of DCE-MRI compared to conventional CE-MRI. Results are also in line with the systematic review of Kwee and Kwee²⁷ who found higher specificity for DCE-MRI compared to standard MRI sequences. Overall, specificity of MRI in surveillance of LR is very important, as a high false positive rate in MRI often leads to unnecessary biopsies for further diagnosis.

Limitations

One limitation is the low number of patients with recurrence. However, recurrence according to the recent literature is only seen in 16% of patients.^{13,28} Further research with a higher number of patients should be performed to substantiate these primarily encouraging results. The required scanning time for DCE-MRI, which increases about 10 minutes the protocol duration for every patient and must be taken into account for economic considerations and also the image evaluation time, which takes approximately 15 minutes to run the software and obtain rPF and rMTT parameters.

Conclusion

Evaluation of rPF with DCE-MRI is a promising quantitative method to differentiate LR in STS of the limb from benign post therapeutic changes. Especially specificity in detection of LR is increased compared to morphological assessment, which might be of clinical relevance as an additional diagnostic method. DWI, however, did not show significantly different ADC values.

Acknowledgment

Open Access funding enabled and organized by Projekt DEAL.

References

1. Stiller CA, Trama A, Serraino D, et al. Descriptive epidemiology of sarcomas in Europe: Report from the RARECARE project. *Eur J Cancer* 2013;49(3):684-695.
2. Casali PG, Abecassis N, Aro HT, et al. Soft tissue and visceral sarcomas: ESMO-EURACAN clinical practice guidelines for diagnosis, treatment and follow-up. *Ann Oncol* 2018;29(Suppl 4):iv51-iv67.
3. Beane JD, Yang JC, White D, Steinberg SM, Rosenberg SA, Rudloff U. Efficacy of adjuvant radiation therapy in the treatment of soft tissue sarcoma of the extremity: 20-year follow-up of a randomized prospective trial. *Ann Surg Oncol* 2014;21(8):2484-2489.
4. Issels RD, Lindner LH, Verweij J, et al. Neo-adjuvant chemotherapy alone or with regional hyperthermia for localised high-risk soft-tissue sarcoma: A randomised phase 3 multicentre study. *Lancet Oncol* 2010;11(6):561-570.
5. Daigeler A, Zmarsly I, Hirsch T, et al. Long-term outcome after local recurrence of soft tissue sarcoma: A retrospective analysis of factors predictive of survival in 135 patients with locally recurrent soft tissue sarcoma. *Br J Cancer* 2014;110(6):1456-1464.
6. Rosenberg SA, Tepper J, Glatstein E, et al. The treatment of soft-tissue sarcomas of the extremities: Prospective randomized evaluations of (1) limb-sparing surgery plus radiation therapy compared with amputation and (2) the role of adjuvant chemotherapy. *Ann Surg Oncol* 1982;196:305-315.
7. Yang JC, Chang AE, Baker AR, et al. Randomized prospective study of the benefit of adjuvant radiation therapy in the treatment of soft tissue sarcomas of the extremity. *J Clin Oncol* 1998;16:197-203.
8. Sabolch A, Feng M, Griffith K, et al. Risk factors for local recurrence and metastasis in soft tissue sarcomas of the extremity. *Am J Clin Oncol* 2012;35(2):151-157.
9. Ezuddin NS, Pretell-Mazzini J, Yechieli RL, Kerr DA, Wilky BA, Subhawong TK. Local recurrence of soft-tissue sarcoma: Issues in imaging surveillance strategy. *Skeletal Radiol* 2018;47(12):1595-1606.
10. Noebauer-Huhmann IM, Weber MA, Lalam RK, et al. Soft tissue tumors in adults: ESSR-approved guidelines for diagnostic imaging. *Semin Musculoskelet Radiol* 2015;19(5):475-482.
11. Roberts CC, Kransdorf MJ, Beaman FD, et al. ACR appropriateness criteria follow-up of malignant or aggressive musculoskeletal tumors. *J Am Coll Radiol* 2016;13(4):389-400.
12. Cheney MD, Giraud C, Goldberg SI, et al. MRI surveillance following treatment of extremity soft tissue sarcoma. *J Surg Oncol* 2014;109(6):593-596.
13. Labarre D, Aziza R, Filleron T, et al. Detection of local recurrences of limb soft tissue sarcomas: Is magnetic resonance imaging (MRI) relevant? *Eur J Radiol* 2009;72(1):50-53.
14. Hirschmann A, van Praag VM, Haas RL, van de Sande MAJ, Bloem JL. Can we use MRI to detect clinically silent recurrent soft-tissue sarcoma? *Eur Radiol* 2020;30(9):4724-4733.
15. Grande FD, Subhawong T, Weber K, Aro M, Mugera C, Fayad LM. Detection of soft-tissue sarcoma recurrence: Added value of functional MR imaging techniques at 3.0 T. *Radiology* 2014;271:499-511.
16. Crombe A, Fadli D, Buy X, Italiano A, Saut O, Kind M. High-grade soft-tissue sarcomas: Can optimizing dynamic contrast-enhanced MRI postprocessing improve prognostic radiomics models? *J Magn Reson Imaging* 2020;52(1):282-297.
17. Geith T, Biffar A, Schmidt G, et al. Quantitative analysis of acute benign and malignant vertebral body fractures using dynamic contrast-enhanced MRI. *AJR Am J Roentgenol* 2013;200(6):W635-W643.
18. Sourbron S, Sommer WH, Reiser MF, Zech CJ. Combined quantification of liver perfusion and function with dynamic gadoteric acid-enhanced MR imaging. *Radiology* 2012;263:874-883.
19. Armbruster M, D'Anastasi M, Holzner V, et al. Improved detection of a tumorous involvement of the mesorectal fascia and locoregional lymph nodes in locally advanced rectal cancer using DCE-MRI. *Int J Colorectal Dis* 2018;33(7):901-909.
20. Landis JR, Koch GG. The measurement of observer agreement for categorical data. *Biometrics* 1977;33(1):159-174.
21. Armbruster M, Sourbron S, Haug A, et al. Evaluation of neuroendocrine liver metastases: A comparison of dynamic contrast-enhanced magnetic resonance imaging and positron emission tomography/computed tomography. *Invest Radiol* 2014;49:7-14.

22. Subhawong TK, Wilky BA. Value added: Functional MR imaging in management of bone and soft tissue sarcomas. *Curr Opin Oncol* 2015; 27(4):323-331.
23. Wang CS, Du LJ, Si MJ, et al. Noninvasive assessment of response to neoadjuvant chemotherapy in osteosarcoma of long bones with diffusion-weighted imaging: An initial in vivo study. *PLoS One* 2013;8(8):e72679.
24. Chodyla M, Demircioglu A, Schaarschmidt BM, et al. Evaluation of (18) F-FDG PET and DWI datasets for the prediction of therapy response of soft tissues sarcomas under neoadjuvant isolated limb perfusion. *J Nucl Med* 2020;62:348-353.
25. Hayashida Y, Hirai T, Yakushiji T, et al. Evaluation of diffusion-weighted imaging for the differential diagnosis of poorly contrast-enhanced and T2-prolonged bone masses: Initial experience. *J Magn Reson Imaging* 2006;23(3):377-382.
26. Choi H, Varm DGK, Fornage BD, Kim EE, Johnston DA. Soft-tissue sarcoma MR imaging vs sonography for detection of local recurrence after surgery. *Am Roentgen Ray Soc* 1991;157:353-358.
27. Kwee RM, Kwee TC. Diagnostic performance of MRI in detecting locally recurrent soft tissue sarcoma: Systematic review and meta-analysis. *Eur Radiol* 2022. <https://doi.org/10.1007/s00330-021-08457-w>
28. Pisters PW, Leung DH, Woodruff J, Shi W, Brennan MF. Analysis of prognostic factors in 1,041 patients with localized soft tissue sarcomas of the extremities. *J Clin Oncol* 1996;14(5):1679-1689.